Available online at www.sciencedirect.com
SCIENCE DIRECT®
Journal of Solid State Chemistry 178 (2005) 2602–2607
JOURNAL OF SOLID STATE CHEMISTRY
www.elsevier.com/locate/jssc

Sb_2O_4 at high pressures and high temperatures

D. Orosel[a], P. Balog[a], H. Liu[b], J. Qian[c], M. Jansen[a,*]

[a] *Max-Planck Institute for Solid State Research, Heisenbergstrasse 1, D-70569 Stuttgart, Germany*
[b] *HP-CAT, Bld. 434E, Advanced Photon Source, Argonne National Laboratory, Argonne, IL 60439-4803, USA*
[c] *LANSCE-12, MS H805, Los Alamos National Laboratory, Los Alamos, NM 87545, USA*

Received 30 March 2005; received in revised form 20 May 2005; accepted 27 May 2005
Available online 20 July 2005

Abstract

Investigations on Sb_2O_4 at high pressure and temperature have been performed up to 600 °C and up to 27.3 GPa. The so-called "high temperature" phase (β-Sb_2O_4) was obtained following pressure increase at ambient temperature and at relatively low temperatures. Thus, in contrast to previous perceptions, β-Sb_2O_4 is the modification more stable at high pressures, i.e., at low temperatures. The fact that the metastable α-form is typically obtained through the conventional way of preparation has to be attributed to kinetic effects. The pressure-induced phase transitions have been monitored by in-situ X-ray diffraction in a diamond anvil cell, and confirmed ex-situ, by X-ray diffraction at ambient conditions, following temperature decrease and decompression in large volume devices. Bulk modulus values have been derived from the pressure-induced volume changes at room temperature, and are 143 GPa for α-Sb_2O_4 and 105 GPa for the β-Sb_2O_4.

Keywords: Antimony oxide; Phase stability; High pressure; High temperature

1. Introduction

The oxides and fluorides of the 14th, 15th and 16th Groups are little known at elevated pressures and temperatures. The common characteristic of these materials is the presence of the non-bonding lone-pair electrons, in many of their binary and tertiary compounds. The reports providing information on the structure, and on the physical and transport properties of such compounds at elevated pressures are rather scarce [1–3], mainly due to their high reactivity. Theoretical models suggest that new electronic properties could be achieved in these structures by applying elevated pressures. In addition, it is long being held that the transformation to a higher density is likely associated with an electronic transition to a metallic behaviour. This is induced by either delocalization of the lone-pair, or by an overlap of the conduction band with the valence band containing the non-bonding pair.

The present report is part of a larger project dedicated to studying the pressure- (p) and temperature (T)-induced mobility of the electron lone-pairs in oxides and fluorides of elements from the 14th, 15th and 16th Groups [4,5]. We have investigated the Sb–O system at elevated pressure and temperature conditions [6]. Four different binary antimony oxides are known to exist at 1 atm and temperatures up to 1250 °C: Sb_2O_3, Sb_2O_4, Sb_6O_{13} and Sb_2O_5 [7]. Literature provides scarce high pressure and high temperature (HP–HT) reports on the Sb–O system, and no data for Sb_2O_4 were found. Therefore, in the present study we report for the first time high-pressure data on the Sb_2O_4 system. In practical applications, Sb_2O_4 is typically used together with other oxides as a catalyst for hydrocarbon cracking and hydrogen reduction, and in the production of ceramic enamels.

The mixed valence Sb_2O_4 contains Sb in the oxidation states +3 and +5, where Sb(III) has a stereochemically

*Corresponding author. Fax: +49 711 689 1502.
E-mail address: m.jansen@fkf.mpg.de (M. Jansen).

0022-4596/$ - see front matter © 2005 Elsevier Inc. All rights reserved.
doi:10.1016/j.jssc.2005.05.037

active lone electron pair. According to literature data, Sb_2O_4 exists in two stable modifications: the room temperature α-Sb_2O_4 [8–12] is orthorhombic $Pna2_1$ (no. 33), with $a = 5.4426(6)$ Å, $b = 4.8098(5)$ Å, $c = 11.7830(13)$ Å, $V = 308.45(9)$ Å^3 and $Z = 4$, while the high temperature β-Sb_2O_4 [10–13] is monoclinic $C2/c$ (no. 15), with $a = 12.0582(1)$ Å, $b = 4.8344(0)$ Å, $c = 5.3827(0)$ Å, $\beta = 104.6°$, $V = 303.65(0)$ Å^3 and $Z = 4$. At 1 atm, the α to β transition is reported to occur at 935 °C [10,14].

2. Experimental details

2.1. Large-volume experiments

The starting sample material of crystalline α-Sb_2O_4 powder was prepared by heating high-purity Sb_2O_3 (Ventron–Alfa Products, ultrapure) in oxygen-flow at 530 °C for 24 h. The obtained powder was ground down, and the whole procedure repeated. The X-ray diffraction patterns obtained (STOE Stadi P instrument with Cu$K_{\alpha1}$ radiation, with a curved Johansson-type monochromator using Ge (111), generating a beam with 1.540598 Å wavelength), showed only reflections corresponding to α-Sb_2O_4.

For the HP–HT experiments, the antimony oxide was packed in tightly closed 4 mm and 2 mm diameter crucibles. Experiments have been performed using a belt-type press (Dieffenbacher GmbH, Germany), and a multianvil press (Voggenreiter GmbH, Germany) equipped with a Walker module. Both presses have been previously *p*- and *T*-calibrated. Temperature was measured with Ni/Cr–Ni thermocouples in the belt runs and with W3Re/W26Re thermocouples in the Walker module. After the experiments, X-ray diffraction patterns of the samples were taken at ambient conditions. All samples containing small amounts of sample holder impurities have been removed from the final analysis.

2.2. Diamond-anvil cell (DAC) experiments

High-pressure synchrotron X-ray experiments were carried out by using a DAC. The *T* 301 stainless steel used as gasket was pre-indented to a thickness of 40 μm from 250 μm, and then a 100 μm diameter hole was drilled in its centre by spark erosion. A thin pre-pressed pellet of powder α-Sb_2O_4 with thickness about 10 μm was loaded into the gasket. Silicone oil, which is chemically inert and could generate quasi-hydrostatic pressure conditions, was used as pressure transmitting medium. Two tiny ruby balls were loaded into the sample chamber as pressure markers for the ruby fluorescence method. The pressure values at each step were determined by averaging the pressure readings measured before and after taking X-ray diffraction patterns. In-situ high-pressure angle-dispersive X-ray diffraction (ADXRD) experiments were performed at room temperature at ID-B station of HPCAT, Advanced Photon Source, Argonne National Laboratory. A double-crystal branching monochromator using water-cooled diamond (111) and Si (220), generated monochromatic beam with wavelength $\lambda = 0.4157$ Å, focussed by multi-electrode modular piezoelectric bimorph mirrors in Kirkpatrick-Baez configurations down to 15 μm diameter. A Mar345 image plate with 100 μm pixel size resolution collected the diffraction patterns, with exposure times between 30 and 150 s. The distance between sample and detector was about 428 mm. Fit2D software [15] was used to integrate the diffraction image. The error in $\delta d/d$ measurement is estimated to be about 10^{-4}, based on the calibration of silicon standard purchased from the National Institute of Standards and Technology.

3. Experimental results

Following the high-pressure runs in large volume presses, the complete transformation of α-Sb_2O_4 into β-Sb_2O_4 was observed at 6 GPa and 375 °C, as seen in Fig. 1. At 4 and 6 GPa, and temperatures between 23 and 350 °C, we noticed the presence of a mixture of α-Sb_2O_4 and β-Sb_2O_4, with a decrease in the quantitative ratio between the two phases induced by temperature increase. At 6 GPa and 400 °C the diffraction pattern indicated β-Sb_2O_4 and a small amount of Sb_2O_3.

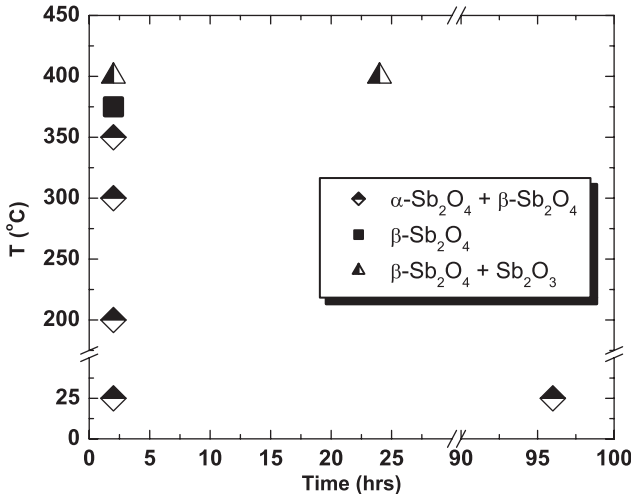

Fig. 1. Result of the high-pressure runs on α-Sb_2O_4, performed at 6 GPa in large volume belt and multianvil presses. The β-Sb_2O_4 seem to be already occurring at 6 GPa and RT, in the 2 h run, indicating that the fast *P*-increase induces the transformation into the more stable phase.

In addition, following runs at 6 GPa and 23 °C, X-ray diffraction analyses revealed the presence of monoclinic β-Sb_2O_4, as shown in Fig. 1. The transformation of the α-phase into β-phase at 6 GPa and ambient temperature is time dependent, but it has a relatively slow kinetics: the amount of the β-phase increased substantially after 24 h, while only traces were found after the 2 h run.

In the DAC experiments performed at 23 °C, the α-Sb_2O_4 started transforming at relatively low pressures, but the complete conversion into β-Sb_2O_4 occurred at pressures much higher than encountered at 375 °C in the large volume presses. The first peaks corresponding to the β-phase appeared at 3.3 GPa (see inset in Fig. 2). Upon further pressure increase, the reflections of the α-phase decrease gradually. Starting at 20 GPa, only the reflections of the β-phase are visible, and the peaks show a strong pressure-induced broadening. In the X-ray pattern, no more changes are seen until reaching the maximum pressure of 27.3 GPa. On pressure release, no signs of a return to the α-phase were detected. Furthermore, after 24 h following pressure decrease to 1 atmosphere, only the β-Sb_2O_4 was detectable in the X-ray pattern.

The DAC experiments provided information regarding the pressure-induced volume changes for the two phases of Sb_2O_4. We used the $p-V$ data to derive the bulk modulus of each individual phase, using the 3rd-order formulation of the Birch–Murnaghan Equation of State (EOS) [16]:

$$p_{BM} = \frac{3}{2} K_{0T}\left[\left(\frac{V_0}{V}\right)^{7/3} - \left(\frac{V_0}{V}\right)^{5/3}\right] \times\left\{1 - \frac{3}{4}(4 - K'_{0T})\left[\left(\frac{V_0}{V}\right)^{2/3} - 1\right]\right\}, \quad (1)$$

where p stands for pressure, V_0 is the volume at $p = 0$, and K_{0T} and K'_{0T} correspond to the bulk modulus and its first pressure derivative, respectively. For this purpose, we employed the EOS fitting program of Angel [17], and we conveniently selected a $K'_0 = 4$. The fitted curves are shown in Figs. 3 and 4. The derived

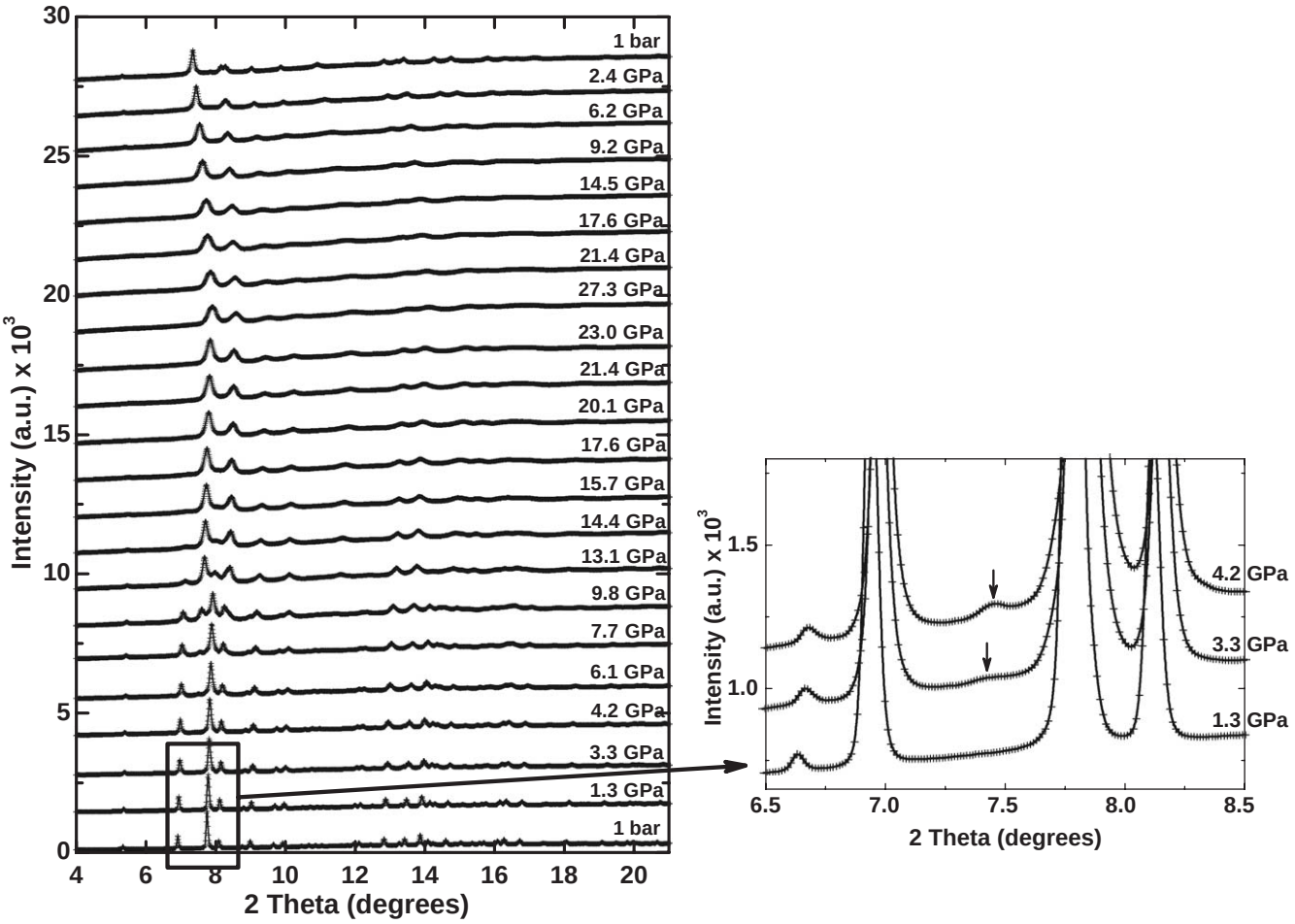

Fig. 2. In-situ X-ray diffraction patterns recorded during pressure increase and decrease at 23 °C in the DAC. The selected region shows the first peaks indicating the occurrence of the β-Sb_2O_4 phase.

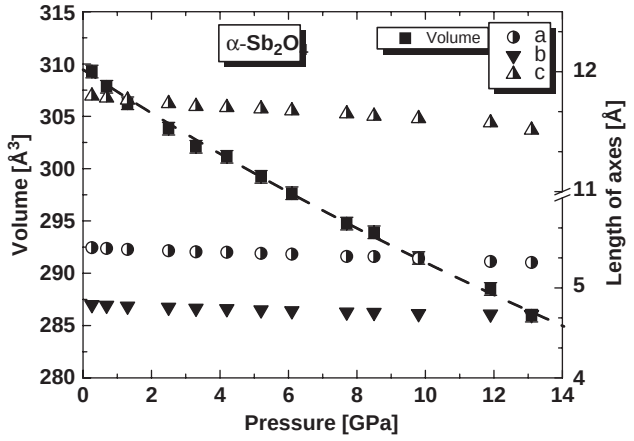

Fig. 3. Pressure-induced changes in lattice size of α-Sb_2O_4 during pressure increase (at 23 °C in the DAC), and the derived change in volume. Dashed line is the fitted isothermal Equation of State.

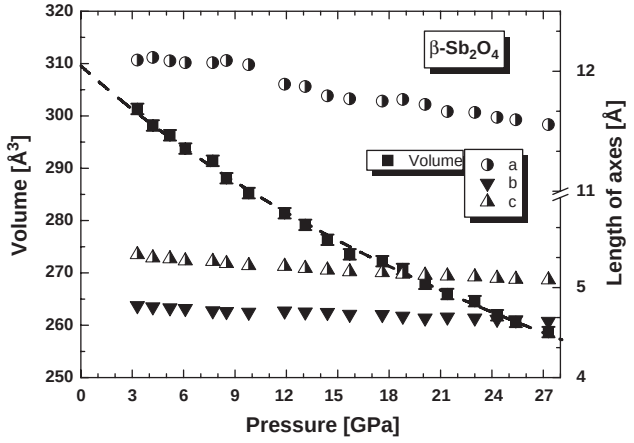

Fig. 4. Pressure-induced changes in lattice size of β-Sb_2O_4 during pressure increase (at 23 °C in the DAC), and the derived change in volume. Dashed line is the fitted isothermal Equation of State.

bulk modulus values for Sb_2O_4 are $K_{0\alpha} = 143 \pm 1.5$ GPa for the α-phase, and $K_{0\beta} = 105 \pm 1.5$ GPa for the β-phase. Similar results were obtained using the Vinet EOS [18]:

$$p_{\mathrm{Vin}} = \frac{3K_{0\mathrm{T}}[1-(V/V_0)^{1/3}]}{(V/V_0)^{2/3}} \times \exp\left[\frac{3}{2}\left(K'_{0\mathrm{T}}-1\right)\left(1-\left(\frac{V}{V_0}\right)^{1/3}\right)\right]. \quad (2)$$

The relatively low value of K_0 obtained for the β-phase is rather atypical for oxides, most of which usually exhibit an increase in K_0 for high-pressure phases with higher density. However, such anomaly is not unique, being also encountered in elemental Si, Pb and FeS (troilite).

4. Crystal structure of the Sb_2O_4 phases

The GSAS software [19] was used for crystal structure refinements of both modifications of di-antimony tetraoxide. The starting values for the refinements of the X-ray diffraction patterns of α- and β-Sb_2O_4 were taken from the single crystal data by Amador et al. [12]. The refined values for the lattice parameters, the atomic positions and the resulting bond lengths were found to be comparable to previous refinements [9–13]. As shown in Figs. 5 and 6, the crystal structure in both modifications is relatively similar, although α-Sb_2O_4 is orthorhombic $Pna2_1$ and β-Sb_2O_4 is monoclinic $C2/c$. The structure consists, in both phases, of distorted $Sb^{V}O_6$ octahedra and $Sb^{III}O_4E$ pyramids.

The connection between the $Sb^{V}O_6$ octahedra is established through sharing of corners and through formation of layers, as shown in Figs. 7 and 8. The octahedra around Sb(V) are in the α-form more distorted than in the β-form. The Sb(III) atoms form

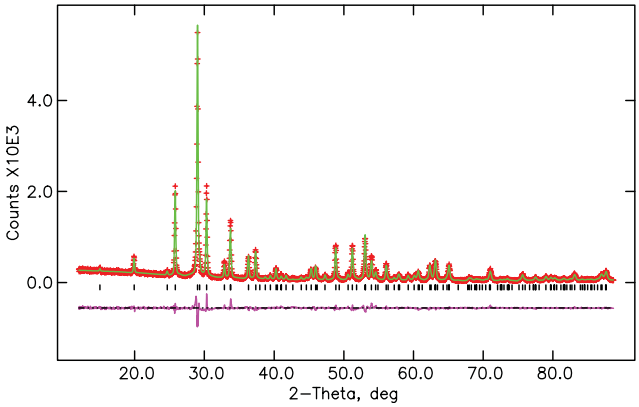

Fig. 5. X-ray diffraction pattern of α-Sb_2O_4 at ambient p, T conditions. Crosses stand for measured data; the line is the calculated pattern. The difference is plotted under the bars representing the positions of the Bragg diffraction peaks.

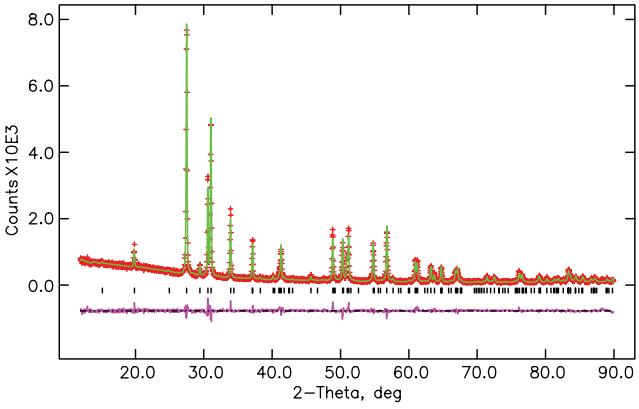

Fig. 6. Ambient conditions X-ray diffraction pattern of β-Sb_2O_4, following a run at 6 GPa and 375 °C. Crosses are the experimental data; the line is the calculated pattern. The difference is plotted under the bars representing the positions of the Bragg diffraction peaks.

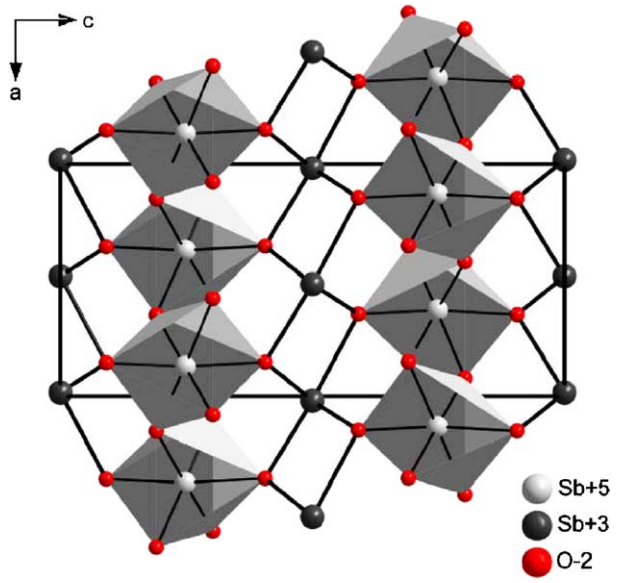

Fig. 7. Structure of α-Sb_2O_4.

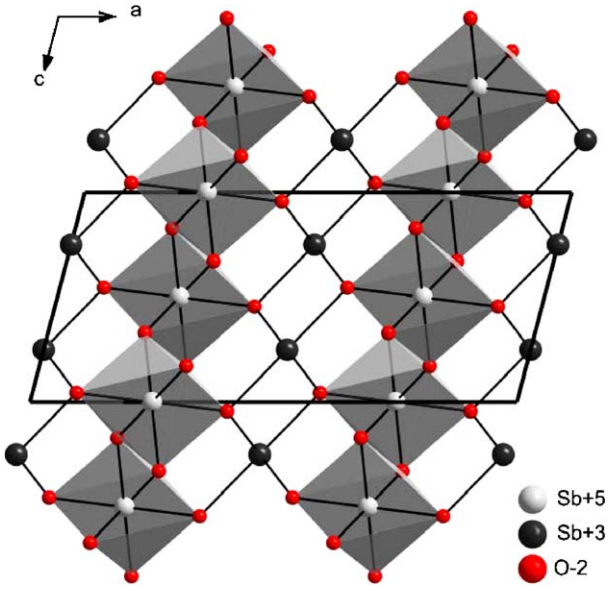

Fig. 8. Structure of β-Sb_2O_4.

rows parallel to these layers and build up the $Sb^{III}O_4E$ units, which share a common edge. Two oxygen atoms belong to the upper layer, and two to the lower layer of the pyramids. The lone electron pair at top of the Sb(III)O_4E pyramids points always in the opposite direction compared to the neighbouring unit.

5. General conclusions

We report here, for the first time, high-pressure and temperature experiments performed on Sb_2O_4. Using both DAC and large volume presses, we determine that the β-modification of Sb_2O_4 is obtained when pressure is applied, under ambient, as well as relatively high temperature. We found the β-phase to be particularly stable at ambient conditions (post quench and decompression), and that the transformation is irreversible, even after heating to temperatures up to 800 °C (T-dependent XRD-runs). Our crystal structure refinement shows, that at ambient p- and T-conditions, β-Sb_2O_4 has a cell volume of $V = 303.62\,\text{Å}^3$ and a density of $\rho = 6.73\,\text{g/cm}^3$. By comparison, the values corresponding to α-Sb_2O_4, which is the actual product of the common way of preparation at 1 atm, are $V = 308.47\,\text{Å}^3$ and $\rho = 6.62\,\text{g/cm}^3$. The result implies that the β-phase is more efficiently packed than α-Sb_2O_4, which until now was assumed to be the more stable one at ambient p and T. Typically, a "high-temperature" modification is expected to have a larger volume and a lower density, in comparison to the room temperature phase. However, according to the outcome of our high temperature (large volume presses) and room temperature (DAC) experiments, we conclude that β-Sb_2O_4 is the thermodynamically stable modification of antimony(III,V) oxide for the entire $p-T$ range covered by the present study. This finding is also supported by the fact that, under elevated pressures and temperatures, Sb_2O_3 is decomposing, forming the β-phase of Sb_2O_4 and elemental Sb [6]. Our results validate the suggestions previously made by Keve and Skapski [20], that the β-phase could be the more stable one, and that it is not expected be revert to the α-phase by heating.

The pressure homology rule [21] specifies that the space group and structure of a high-pressure phase should be similar to the space group of the analogues compound of the next heavier element in the same group at ambient conditions. Bismuth(III,V) oxide, which is monoclinic $C2/c$ and is a structural analogue of β-Sb_2O_4, was synthesized by Kumada et al. [22] at ambient pressure. Apparently, the rule should be applicable for β-Sb_2O_4 and Bi_2O_4: both have the same structure, and the β-form of Sb_2O_4 could be obtained by applying high pressure. However, the α to β transition is also temperature induced, and the α-Sb_2O_4 is not recovered by cooling the β-modification. Since in both cases, Sb_2O_4 and Bi_2O_4, the modifications stable at ambient conditions are isostructural, the pressure homology rule does not apply.

Acknowledgments

This work was supported by the Max-Planck Society and by a grant from Fonds der Deutschen Chemischen Industrie to M. Jansen. We thank F. Falkenberg for help with the preparation of high-pressure cells and experiments.

Appendix A

Tables of the refined crystallographic data (Tables 1 and 2).

Table 1
Room temperature crystallographic and least-square refinement data for α-Sb_2O_4 (before *P*-increase, at 0 and 9.8 GPa) and β-Sb_2O_4 (at 9.2 and 0 GPa, following *P*-decrease)

(a)

α-Sb_2O_4	0 GPa	9.8 GPa
Space group	$Pna2_1$ (no. 33)	$Pna2_1$ (no. 33)
Unit cell dimensions (Å)	$a = 5.4524(1)$ $b = 4.8180(1)$ $c = 11.8083(2)$	$a = 5.3336(17)$ $b = 4.7138(15)$ $c = 11.6146(27)$
Cell volume (Å^3)	$V = 310.20(1)$	$V = 292.01(15)$
Z	4	4
Density (g/cm^3)[a]	6.584	6.994
Least-square refinement data (%)[b]		
wR_p	1.17	2.54
R_p	0.71	1.39
R (F^2)	5.82	13.12

(b)

β-Sb_2O_4	0 GPa	9.2 GPa
Space group	$C2/c$ (no. 15)	$C2/c$ (no. 15)
Unit cell dimensions (Å)	$a = 12.1155(22)$ $b = 4.8465(8)$ $c = 5.4014(11)$ $\beta = 104.59(1)^\circ$	$a = 11.8960(18)$ $b = 4.7567(15)$ $C = 5.2449(17)$ $\beta = 106.73(3)^\circ$
Cell volume (Å^3)	$V = 306.93(10)$	$V = 284.22(25)$
Z	4	4
Density (g/cm^3)[a]	6.654	7.186
Least-square refinement data (%)[b]		
wR_p	0.86	0.56
R_p	0.51	0.41
R (F^2)	15.37	11.97

[a]Calculated values
[b]As given in the GSAS manual.

Table 2
Atomic positions and thermal parameters of α-Sb_2O_4 and β-Sb_2O_4, following Rietveld refinement of DAC data during *P*-increase (for the α-phase) and *P*-decrease (for the β-phase), for similar pressure ranges. Refined were lattice parameters, atomic positions, parameters of the profile function and background function

Atom	Site	X	Y	Z	U_{iso} (Å^2)
α-Sb_2O_4	$P = 0$ GPa/$V = 310.20$ Å^3				
Sb1 (+5)	4*a*	0.37408(28)	0.9972(20)	0.2455(6)	0.0005
Sb2 (+3)	4*a*	0.9803(8)	0.0352(4)	0.0010(6)	0.0081(9)
O1	4*a*	0.338(4)	0.140(4)	0.0879(11)	0.0020
O2	4*a*	0.1592(22)	0.6919(23)	0.1883(13)	0.0020
O3	4*a*	0.0708(23)	0.2129(28)	0.3133(11)	0.0020
O4	4*a*	0.341(4)	0.806(4)	0.4006(12)	0.0020
α-Sb_2O_4	$P = 9.8$ GPa/$V = 292.01$ Å^3				
Sb1 (+5)	4*a*	0.3775(23)	1.006(7)	0.2449(16)	0.043(7)
Sb2 (+3)	4*a*	0.9475(31)	0.0530(26)	0.0018(23)	0.045(8)
O1	4*a*	0.266(12)	0.147(20)	0.090(4)	0.0020
O2	4*a*	0.093(10)	0.791(14)	0.180(4)	0.0020
O3	4*a*	0.178(7)	0.318(10)	0.315(4)	0.0020
O4	4*a*	0.354(13)	0.833(19)	0.4056(33)	0.0020
β-Sb_2O_4	$P = 0$ GPa/$V = 306.93$ Å^3				
Sb1 (+5)	4*c*	1/4	1/4	0	0.020(4)
Sb2 (+3)	4*e*	0	0.2900(17)	1/4	0.060(7)
O1	8*f*	0.1854(18)	−0.052(6)	0.749(6)	0.0020
O2	8*f*	0.1067(15)	0.413(5)	1.036(5)	0.0020
β-Sb_2O_4	$P = 9.2$ GPa/$V = 284.22$ Å^3				
Sb1 (+5)	4*c*	1/4	1/4	0	0.0110(23)
Sb2 (+3)	4*e*	0	0.2791(16)	1/4	0.087(5)
O1	8*f*	0.1742(12)	−0.052(4)	0.7363(34)	0.0020
O2	8*f*	0.0993(11)	0.395(4)	1.0165(34)	0.0020

References

[1] U. Häussermann, P. Berastegui, S. Carlson, J. Haines, J.-M. Leger, Angew. Chem. Int. Ed. 40 (2001) 4624.
[2] D. Becker, H. Beck, Z. Kristallogr. 219 (2004) 348.
[3] X. Wang, F. Zhang, I. Loa, K. Syassen, M. Hanfland, Y.-L. Mathis, Phys. Stat. Sol. B 241 (2004) 3168.
[4] D. Orosel, O. Leynaud, P. Balog, M. Jansen, J. Solid State Chem. 177 (2004) 1631.
[5] R. Dinnebier, S. Carlson, M. Hanfland, M. Jansen, Am. Mineral. 88 (2003) 996.
[6] D. Orosel, P. Balog, M. Jansen, New phases of Sb_2O_3 under high pressures and high temperatures, in preparation.
[7] T.B. Massalski (Ed.), Binary Alloy Phase Diagrams, second ed., vol. 3, ASM International, Materials Park Ohio, 1990, pp. 2912–2913.
[8] W. Gründer, H. Pätzold, H. Strunz, Neues Jahrb. Min. 5 (1962) 93.
[9] K. Dihlström, Z. Anorg. Allg. Chem. 239 (1938) 57.
[10] D. Rogers, A.C. Skapski, Proc. Chem. Soc. (1964) 400–401.
[11] G. Thornton, Acta Crystallogr. B 33 (1977) 1271–1273.
[12] J. Amador, E. Gutierrez Puebla, M.A. Monge, I. Rasines, C. Ruiz Valero, Inorg. Chem. 27 (1988) 1367–1370.
[13] R. Basso, G. Lucchetti, L. Zefiro, A. Palenzona, Eur. J. Mineral. 11 (1999) 95–100.
[14] R.G. Teller, M.R. Antonio, J.F. Brazdil, M. Mehicic, R.K. Grasselli, Inorg. Chem. 24 (1985) 3370–3375.
[15] A.P. Hammersley, S.O. Svensson, M. Hanfland, A.N. Fitch, D. Häusermann, High Pressure Res. 14 (1996) 235–248.
[16] F.D. Murnaghan, Am. J. Math. 59 (1937) 235–260.
[17] R.J. Angel, EOS-FIT v.5-2, www-freeware, Virginia Tech., 2001–2003.
[18] P. Vinet, J. Ferrante, J.R. Smith, J.H. Rose, J. Phys. C 19 (1986) L467–L473.
[19] C. Larson, R.B. Von Dreele, General Structure Analysis System (GSAS), Los Alamos National Laboratory Report LAUR, 2000, pp. 86–748.
[20] E.T. Keve, A.C. Skapski, J. Solid State. Chem. 8 (1973) 159–165.
[21] A. Neuhaus, Chimia 18 (1964) 93–103.
[22] N. Kumada, N. Kinomura, P.M. Woodward, A.W. Sleight, J. Solid State Chem. 116 (1995) 281–285.